



**DYNAMIC POSITIONING CONFERENCE**  
October 13 – 14, 1998

**DESIGN**

---

Physical Model Testing of Floating  
Offshore Structures

**Subrata Chakrabarti**  
*Offshore Structure Analysis, Inc.*

---

## TABLE OF CONTENTS

<b>Abstract.....</b>	<b>2</b>
<b>1.0 INTRODUCTION.....</b>	<b>2</b>
<b>2.0 MODELING CRITERIA.....</b>	<b>3</b>
<b>2.1 Scaling Laws.....</b>	<b>3</b>
<b>2.2 Froude Similitude.....</b>	<b>3</b>
<b>2.3 Strouhal Similitude.....</b>	<b>4</b>
<b>2.4 Reynolds Similitude.....</b>	<b>4</b>
<b>2.5 Cauchy Similitude.....</b>	<b>5</b>
<b>2.6 Modeling Technique.....</b>	<b>6</b>
2.6.1 Modeling of Floater.....	6
2.6.2 Modeling of Mooring Line.....	6
2.6.3 Modeling of Risers.....	7
<b>3.0 DEEP WATER MODEL TESTING.....</b>	<b>7</b>
<b>3.1 Requirements of a Test Facility.....</b>	<b>7</b>
3.1.1 Physical Dimensions.....	7
3.1.2 Towing Carriage and Planar Motion Mechanism.....	8
3.1.3 Instrumentation.....	8
3.1.4 Six D.O.F. Mechanical System.....	8
3.1.4 Towing Dynamometry.....	9
<b>4.0 MODELING OF ENVIRONMENT.....</b>	<b>9</b>
<b>4.1 Wave Generation.....</b>	<b>9</b>
<b>4.2 White Noise Seas.....</b>	<b>10</b>
<b>4.3 Wave Grouping.....</b>	<b>10</b>
<b>4.4 Wind Generation.....</b>	<b>11</b>
<b>4.5 Current Simulation.....</b>	<b>12</b>
<b>5.0 AREAS OF TESTING.....</b>	<b>13</b>
<b>5.1 Air Gap Measurement.....</b>	<b>13</b>
<b>5.2 Motion Measurement.....</b>	<b>13</b>
<b>5.3 Sectional loads.....</b>	<b>13</b>
<b>5.4 Towing Tests.....</b>	<b>14</b>
5.4.1 Scaling Up of Towing Load.....	14
5.4.2 Scaling Up of Drag Force.....	15
5.4.3 Turbulence Stimulator.....	15
5.4.4 Towing vs Current.....	15
<b>5.5 Moored System Tests.....</b>	<b>16</b>
<b>5.6 Second Order Slow Drift Tests.....</b>	<b>17</b>
<b>6.0 CONCLUDING REMARKS.....</b>	<b>18</b>
<b>7.0 REFERENCES.....</b>	<b>18</b>

## **Abstract**

The purpose of this paper is to discuss the sea-keeping and towing tests of an offshore structure on station or in transit. Since a small replicate of the prototype is used, several simulation difficulties are experienced in the small scale testing. A few of the difficulties of these tests and the remedial measures used in the setup and in the scaling up of the model data are discussed here. The areas where good correlation is found with the available design tools and the field data are noted.

Small scale physical modeling of a new concept is extremely worthwhile. It is, however, a challenge with the availability of limited large and deepwater basins. Modeling of floating moored system is difficult since complete modeling at a reasonable scale is a difficult task. For example, an FPSO with a spread mooring system for water depths near 2000m may be completely modeled only at a scale of 1:200 or smaller based on the limitation of existing facilities. Therefore, some distortion in the modeling of these systems is unavoidable.

Another area of uncertainty is the effect of Reynolds number. The Reynolds number in a Froude model is smaller by more than an order of magnitude. The distortion of Reynolds number in the model necessitates certain corrective measures in the model tests and scaled data. Use of some of these techniques and the quantitative difference in the results with and without a stimulator for an offshore structure model is shown.

The powering requirements of and current loads on a floating vessel are determined by towing the model in the basin. The towing staff attached to the towing carriage generally allows the vessel to heave and pitch about the attachment point on the vessel, but restrains its motion in the transverse direction. Offshore structures, however, are also towed in a restraint position, or with the mooring system attached, such as, in the simulation of current drag on the in-place structure.

## **1.0 INTRODUCTION**

Offshore exploration and production of minerals is advancing into deeper water at a fast pace. Many deepwater structures have already been installed in waters of the world. New oil/gas fields are being discovered in deep water. Many of these fields are small and the economic development of these fields is a challenge today to the offshore engineers. This has initiated development of new structures and concepts. Many of these structures are unique in many respects and their efficient and economic design and installation are a challenge to the offshore community. In order to meet the need for offshore exploration and production of oil/gas, a new generation of semisubmersible and drillships are being developed.

The purpose of this paper is to investigate the state-of-the-art in the physical simulation and scaling up of the test data of some of the innovative offshore/ marine structures of today. The pros and cons of designing a model test of a free and moored floating structure are discussed.

The need and adequacy of model tests for these structures in light of the physical limitation of testing facilities are addressed. It is recognized that much have been written on this subject. It is not the intent of this paper to repeat these areas. The reader is referred to the textbook by Chakrabarti (1994) for an introduction and details of physical modeling. We intend to highlight the areas of the model-testing role in light of the current development of floating structures.

## 2.0 MODELING CRITERIA

One of the first and foremost tasks in planning a model test is to investigate the modeling laws required for the system in question to be analyzed. This section addresses the scaling parameters that are important in designing a model test and a few key areas of consideration in replicating a prototype structure for a physical model test.

### 2.1 Scaling Laws

In order to achieve similitude between the model and the real structure, the following must be satisfied which are elaborated later:

- Geometric similitude
- Hydrodynamic similitude (Froude, Strouhal and Reynolds)
- Structural similitude (Cauchy)

### 2.2 Froude Similitude

Froude's law is the most appropriate scaling law for the free and moored floating structure tests. The model is usually scaled following Froude's Law. The Froude number has a dimension corresponding to the ratio of  $u^2 / gD$  where  $u$  is the fluid velocity,  $g$  is the gravitational acceleration and  $D$  is a characteristic dimension of the structure. The Froude number  $Fr$  is defined as

$$Fr = \frac{u^2}{gD} \quad [1]$$

Assuming a model scale of  $\lambda$  and geometric similarity, the Froude model must satisfy the relationship:

$$\frac{u_p^2}{gD_p} = \frac{u_m^2}{gD_m} \quad [2]$$

where the subscripts  $p$  and  $m$  stand for prototype and model respectively and  $I$  is the scale factor. According to geometric similarity, the model linear dimensions will be scaled linearly with the scale factor,

$$l_p = I l_m \quad [3]$$

Then, from Eq. 2:

$$u_p = \sqrt{I} u_m \quad [4]$$

Other variable quantities of importance are derived from Eqs. 3 and 4 and dimensional analysis as follows:

$$\text{Mass} \quad m_p = I^3 m_m \quad [5]$$

$$\text{Force} \quad F_p = \frac{I^3}{0.975} F_m \quad [6]$$

The quantity 0.975 is the ratio between the fresh water and sea-water densities.

$$\text{Fluid Acceleration} \quad \dot{u}_p = \dot{u}_m \quad [7]$$

$$\text{Time} \quad t_p = \sqrt{I} t_m \quad [8]$$

$$\text{Stress/Pressure} \quad s_p = I s_m \quad [9]$$

where  $u$ ,  $\dot{u}$ , and  $F$  are the velocity, acceleration and force respectively.

### **2.3 Strouhal Similitude**

Strouhal (Keulegan-Carpenter number) similitude provides the similitude of the unsteady fluid flow. It requires that

$$\frac{u_p T_p}{L_p} = \frac{u_m T_m}{L_m} \quad [10]$$

where  $T$  is the period of oscillation. Note that the Froude similitude also satisfies the Strouhal similitude, which gives

$$\text{Frequency} \quad f_p = f_m / \sqrt{I} \quad [11]$$

### **2.4 Reynolds Similitude**

While the Froude number is a primary scaling parameter in these types of model tests and is used in determining the structure responses, the Reynolds number (Re) effect is not scaled properly in a small scale model. In fact, the Reynolds number (Re) for a Froude model is smaller by a factor of  $\lambda^{1.5}$ .

$$\text{Re}_p = I^{3/2} \text{Re}_m \quad [12]$$

Therefore for a scale factor of  $\lambda = 44$ , the prototype Re is 292 times that of the model Re. The consequence of this difference is that while the prototype flow regime is turbulent, that of the model may necessarily become laminar. The drag coefficients in a laminar flow are normally higher than those found in a turbulent flow. The scaling then is generally expected to be conservative if no corrective measure is taken in scaling. On the other hand, the non-linear damping will produce smaller model response. In spite of this limitation, the resistance of a floating structure in transit or in the presence of current is commonly determined by the towing test of a small scale model. It is obvious that larger the model, the smaller is this distortion. However, the order of the Reynolds number distortion is still quite high.

In order to rectify this deficiency it is a common practice to artificially stimulate turbulence in a model test by introducing roughness in the flow approaching the surface of the model. This stimulation is introduced by attaching studs or sandpaper near its bow for a ship. The stimulation is sometimes added by placing a submerged grid made of a frame of wires or of wood strips. The frame is located a few feet in front of the model on the same carriage used to tow the model thus causing turbulence in the flow just ahead of the model. This addition provides the effect of higher Reynolds number on the resistance and the simulation of flow is closer to the prototype in spite of the Re distortion. For small grid members (e.g., 1/8 inch diameter) the drag-induced velocity from the grid will be quite small.

In combined wave plus simulated current tests, the turbulence in the tank from a confused sea simulation will correct some of the Reynolds distortion in the small scale test. Any submerged square members will provide additional turbulence along their edges in the model flow. The purpose of incorporating the wind and current in a model test is not to scale their effect with respect to the prototype, but to be able to include them to study their interaction with the waves and the structure and use the model values to correlate the design tools.

## 2.5 Cauchy Similitude

In traditional model testing, the model is considered a rigid structure and the model deformation and associated interaction with waves is ignored. While this approach is generally acceptable, for structures that are long or for mooring systems in conjunction with a floating structure such simplification is not acceptable. This coupling of external load with structure response is termed hydroelasticity.

Hydroelasticity deals with the problems of fluid flow past a submerged structure in which the fluid dynamic forces depend on both the inertial and elastic forces on the structure. It is well known that for long slender structures, the stiffness of the structure is important in measuring the response of the structure model in waves.

It is often desired to test structures to determine stresses generated in its members due to external forces, for example, from waves. In this case the elasticity of the prototype should be maintained in the model. Therefore, in addition to the Froude similitude, the Cauchy similitude is desired.

Consider the longitudinal bending. It is desired that this bending should be the same between the model and the prototype. Then,

$$(My/EI)_p = (My/EI)_m \quad [13]$$

in which  $EI$  = flexural rigidity,  $E$  = Young's modulus,  $M$  = vertical bending moment,  $y$  = distance to the outer fiber from the neutral axis. Noting that the bending moment in a Froude model scales as  $\lambda^4$ , the Cauchy similitude requires that stiffness such as in bending of a model must be related to that of the prototype by the relation:

$$(EI)_p = I^5 (EI)_m \quad [14]$$

where  $I$  = moment of inertia. This provides the deflection in the model which is  $1/I$  times the deflection in the prototype; also, stress must be similarly related, such that,  $s_p = I s_m$ , (Froude's law). For example, for a cantilever beam the maximum deflection is given by  $d_{\max} = Pl^3/(3EI)$  where  $P$  is the load at the end of the cantilever of length  $l$ . Equation 13 satisfies Froude's law for this relationship.

Since the section moment of inertia satisfies

$$I_p = I^4 I_m \quad [15]$$

we have:

$$E_p = \lambda E_m \quad [16]$$

Thus, the Young's modulus of the model material should be  $1/\lambda$  times that of the prototype. Assuming that the prototype is made of steel whose Young's modulus is  $E_p = 30 \times 10^6$  psi and  $\lambda=36$ , the model  $E_m$  should be 833,000 psi.

In these cases, an elastic model, which properly takes into account the scale effects is designed and constructed. Sometimes it is not possible to build an elastic model due to lack of suitable material, scaling problem, etc. Often in these cases, a segmented model can be built, where individual segments are properly modeled and the segments are then hinged together with rigid intermediate sections. The elasticity (such as, in bending) is imposed at the hinges. The number and stiffness of these hinges are chosen to provide the scaled mode shapes of the model at its scaled natural frequencies.

In a torsional mode, the similitude condition similarly gives

$$(GI)_p = \lambda^5 (GI)_m \quad [17]$$

where  $GI$ = torsional rigidity. Then, for a model with significant bending and torsional deflection, the model should additionally satisfy

$$G_p = \lambda G_m \quad [18]$$

This is not an easy task to model bending and torsion simultaneously with one material.

## **2.6 Modeling Technique**

Some of the common structure components are modeled as follows:

### **2.6.1 Modeling of Floater**

The geometry of the floater is scaled dimensionally correct for the scale factor. All the dynamic properties, (e.g. displacement, moment of inertia, GM, natural periods) are properly scaled using Froude's law. The structural properties (e.g. elasticity) are not necessary to scale. Even at a small scale (e.g.  $\lambda = 100 - 200$ ), this scaling can provide reasonable results. Many of the details, e.g., appendages and small members, however, are often omitted.

### **2.6.2 Modeling of Mooring Line**

There are three parameters that are important for the floating structure response in terms of the mooring line behavior. They are

- mooring line pretension
- stiffness of the mooring with respect to the environmental load
- The load experienced by the structure at the fairlead from the mooring line under various loading

If these quantities are modeled properly for a given environment then the simulation of the structure response will be properly scaled even though the mooring lines are not physically modeled. It is understood that the interaction of the deepwater mooring lines with the waves can not be modeled in small scale.

An example of the stiffness characteristics of a mooring line for a floating structure is given in Fig. 1. If three spring components are used to simulate this non-linear stiffness, all three spring components acting in series simulate the lowest slope portion of the load-deflection curve. At the transition tension at which the lowest slope

line changes to the next higher slope line, a cable or string is tied between the ends of the weakest spring. This prevents the spring from extending at higher tensions, resulting in a higher spring constant due to one less spring extending in series. This higher spring constant equals the slope of the next line segment of the load-deflection curve. Similarly, at the highest transition tension, the second spring is tied off, so that at higher tension, only the third and strongest spring is actively stretching, with a spring constant matching the highest-slope portion of the load-deflection curve. Additional springs in line are introduced as needed to get a better match to the curve.

Distortion due to truncation in the mooring line length is provided by additional springs. External means of correcting for the damping effect on the line itself from its motion may be introduced in the model chain.

### 2.6.3 Modeling of Risers

For a taut mooring system, the elasticity of a cable/wire (tensile stiffness) is an important property that can be scaled with a suitable material at a small scale.

The risers may be modeled by metal or plastic tubing or other smooth surface material with sufficient rigidity and of the required diameter. Sometimes, an equivalent diameter with the same overall drag area as the total riser array and proper stiffness for a group of risers is simulated. Where the interference effect among the risers is an important area of investigation, all individual risers from the deck to the ocean floor are needed to model. The riser system is subject to a constant tension, which may be provided by a tensioned spring.

## **3.0 DEEP WATER MODEL TESTING**

There are several testing basins in the world that can handle model testing of these systems. Limitation of 10 m overall depth of wave basins for physical testing of these systems is, however, being felt. This is giving rise to virtual reality model basin using Computational Fluid Dynamics (CFD) and 3-D graphics. While the realistic nature of these pictures may be questioned for a long time to come, some believe that they will eventually replace physical model testing. Until such times, physical model testing will remain a strong viable alternative. It should also be noted that the knowledge that is experienced from physical model testing, can not be gained by the numerical model.

### **3.1 Requirements of a Test Facility**

The ultimate goal of a model test is to obtain reliable results that can be scaled up and correlated with analytical design tools. A database on available facilities appropriate for deepwater floating structure tests is included in Table 1. The physical dimensions and some of their capabilities are given in the table from available data. The telephone number is included where available.

#### 3.1.1 Physical Dimensions

In today's development of the deepwater fields, it is desirable to have a deep model basin. In fact, for ultradeep water an extremely deepwater facility is required which is not available. Even the deepest basin in the world is not adequate for the practical simulation of the water depth and the full mooring system simulation. Therefore, it is recognized that some distortion in scaling all the important parameters of a model is inevitable.

It is therefore important to have a test facility that has a variety of options for testing a deepwater floating structure. The facility should be reasonably deep for a reasonable scale of the structure itself and should have the capability to generate waves, current, and wind. It should also have the towing, maneuvering (e.g., through a

Planar Motion Mechanism), and underwater video documentation capability. The preferred requirements for instrumentation and measurements are described later.

### 3.1.2 Towing Carriage and Planar Motion Mechanism

The availability of a towing carriage allows for the current test. For moored structures, an alternative to including the current on the moored system is to tow the entire structure with the mooring system attached to it. In this case the structure installed with mooring lines is mounted on a suitable structural framework which is attached to the carriage. The framework is made transparent so that their effect on the flow field is minimal. Sometimes, the members of the framework are faired for minimum separation of flow.

In towing tests the simulation of current is possible only for a uniform current. The uniformity of this current is superior to any other method of direct physical simulation of current in the basin.

Besides the maneuvering tests, the Planar Motion Mechanism on the carriage allows tests of mechanical simulation of offshore structures, risers or tendons, which is often important. In this case, the model is attached to the PMM and allowed to undergo prescribed motions simulating the dynamic motion of the structure in waves.

### 3.1.3 Instrumentation

The following standard instruments are often required during a test:

- Wave Probes
- Linear and Angular Potentiometers
- Six D.O.F. Mechanical System
- Optical Tracking System
- Single Component (Ring Gauged) Load Cells
- 3 Component Load Cells
- Accelerometers
- Pressure Gauges
- Towing Speed Indicator
- Towing Dynamometer
- Rotating Dynamometer

Instruments for the measurement of responses at a small scale may pose a problem due to its size compared to the model. However, many small precise and reliable instruments are available today. The measurement accuracy or instrument sensitivity at a small scale, say 1:100, is not a serious problem. What creates the inaccuracy in the system is the introduction of superfluous physical phenomenon not present in a larger scale model or prototype, for example, capillary wave effect, etc. The generally accepted overall measurement accuracy is about 5 percent. At a much smaller scale, this accuracy may drop down to as much as 20 per cent. For a small scale testing, this measurement error must be recognized and considered in the correlation and extrapolation of data.

### 3.1.4 Six D.O.F. Mechanical System

The mechanical system of motion measurement uses linkages and linear and angular potentiometers attached between the overhead carriage structure and the model. The measured channels are converted to the six motions of the model at its CG during post processing of the data. If this system is employed, it is important that its effect on the structure in terms of the overall inertia and damping introduced by the mechanical system be known.

### 3.1.4 Towing Dynamometry

A hinge point is generally provided between the towing staff and the dynamometer such that it allows the freedom of the model to pitch and is designed to restrain the model in sway and yaw. The staff is located at or near the CG of the model free to move in the heave direction, but restrained in surge, sway, roll and yaw. In a two staff arrangement the second staff is located aft of the CG of the model and is free to heave and pitch. Often both staffs are rigidly connected to the model, which is then restrained from motion.

The dynamometer at the end of the staff attached to the model measures the resistance and side force. Vertical potentiometers are mounted on the heave staffs to measure the trim (and pitch) and the dynamic sinkage (and heave). In a two staff arrangement, it is preferred to instrument both staffs in this way.

## **4.0 MODELING OF ENVIRONMENT**

The general requirements on the environmental simulation at a wave basin for typical floating structure tests are discussed in the following sections.

### **4.1 Wave Generation**

The frequency band for ocean waves of importance to the offshore structure lies in the range of 5 to 24 seconds. The maximum energy of the ocean waves falls in the area of 10 to 16 seconds. Therefore the model basin should have the capability of generating these waves at a suitable scale with maximum heights in the above range. The model basins should have this information (e.g., Fig. 2) available for its clients. This parameter is very important in determining the suitable scale for a model test

Generation of high frequency wave components at a small scale is difficult in a wave tank. For example, at a scale of 1:100, a 0.5s model wave represents a 5s-prototype wave. Wave generators seldom have quality wave generation capability much below 1 Hz. Waves at 4 -7s may have significant effect on the dynamic response of floating structures. Scales smaller than 1:70 will not allow reproduction of these waves.

Waves in the basin should be calibrated without the presence of the model. The random waves should be generated from the digital time history signal computed from the desired spectral model and the generated spectra should be matched with the theoretical (e.g., P-M or JONSWAP) spectral models. Once an acceptable match is found (e.g., Fig. 3), the setting will be saved for later use. This will assure repeatability of the wave spectrum from one run to the next. Sufficient duration for the random waves and white noise will be given during the test runs so that reliable estimates of the spectra and transfer functions may be made.

Irregular sea state records should allow a test duration of 20 minute (prototype) for irregular test data. For slow drift tests a sea state duration of 120 minutes (prototype) is recommended.

The tolerances for the wave parameters are expected as follows:

#### **Regular Waves**

- Average wave height  $H$ , of a wave train consisting of at least 10 cycles: Tolerances:  $\pm 5\%$
- Average zero-up-crossing wave period  $T$ : Tolerances:  $\pm 0.2$  sec full scale.

#### **Irregular Waves**

- Significant wave height  $H_s$ : Tolerances:  $\pm 5\%$
- Spectral peak period  $T_p$ : Tolerances:  $\pm 0.50$  s full scale.

- Significant part of the measured spectrum shape: maximum  $\pm 10\%$  off

The following spectral formulations may apply for the test program.

JONSWAP Irregular Seas

$$S(f) = \alpha g^2 (2\pi)^{-4} f^{-5} \exp.(-1.25[f/f_p]^{-4}) \gamma^{\exp.(-(f - f_p)^2 / (2\sigma^2 f_p^2))} \quad [19]$$

where  $f$  = frequency, Hz,  $f_p$  = frequency of spectral peak, Hz,  $g$  = acceleration due to gravity,  $\alpha$  = Phillips constant,  $\sigma$  = spectral width parameter,  $\gamma$  = peakedness parameter and  $\sigma = \sigma_A$  for  $f \leq f_p$ ,  $\sigma = \sigma_B$  for  $f > f_p$ .

The Phillips constant,  $\alpha$ , is normally taken as 0.0081 and the width parameters as 0.07 and 0.09 respectively. In general, they are dependent on the significant height and peak periods. For long period wave spectra ( $\gamma \leq 1.0$ ) the spectra may be simplified to the Pierson Moskowitz spectral formulation.

#### **4.2 White Noise Seas**

White noise spectra denote wave spectra with near uniform energy over the full range of wave frequency of interest. Sufficient energy content is required from say 5 to 20 seconds prototype to obtain significant motion response of the structure. This allows to spectrally analyze the response signal and develop response transfer functions, phases and coherence over the given wave period range. The method of data reduction is straightforward with the help of cross-spectral technique [Bendat and Piersol (1980)].

The generation of white noise with significant amount of energy over a wide band of frequencies is a difficult task at any model basin. Therefore, the energy level is necessarily low. Thus, the response will be expected to be small. What may make the data reduction difficult is that most floating structures will respond to the white noise with a slow drift oscillation of significant amount. This will require possible digital filtering of data at the low frequencies. The cross-spectral analysis may not need filtering and the reliable range of transfer function is determined from the high value of coherence. The areas of low coherence are eliminated from the RAO.

Generally, this method provides reasonable accuracy and has the advantage of obtaining the transfer function from one single test run. However, it is recommended that at least limited numbers of regular waves be tested to verify these values of RAO.

#### **4.3 Wave Grouping**

The motions of floating structures are found to be sensitive to wave groups. The wave group is defined by the envelop wave of the square of the wave elevation. The slow drift oscillation is shown to differ significantly by the groupiness present in the irregular wave. Therefore it is important to model the groupiness function in the generated wave in addition to the spectral shape. The groupiness function is computed from the squared integral of the spectral density.

$$G(\mathbf{m}) = 8 \int_0^{\infty} S(\mathbf{w})S(\mathbf{w} + \mathbf{m})d\mathbf{w} \quad [20]$$

in which  $G$  is the groupiness function,  $\omega$  is the circular frequency and  $S$  is the spectral energy density of the irregular wave. This function should be computed for both the spectral model and the simulated wave during its calibration. The two should be matched as closely as possible to insure proper grouping of waves for the slow drift oscillation tests. An example of the comparison of the groupiness function for a JONSWAP wave is shown in Fig. 4.

#### 4.4 Wind Generation

Once the topside layout is finalized the wind tunnel tests will confirm the wind loads on the topside. However, the steady wind load measured in a wind tunnel test will have small effect on the overall performance of the model dynamics in the wave tank. It is often suffices to duplicate the computed wind loads on the model superstructure during the wave tank tests. The generation of wind is often accomplished by a simulated weight representing the steady load from the wind applied with a string and pulley arrangement at the center of application of the superstructure. This arrangement provides the proper tension in the mooring system, but fails to simulate the variation of the wind spectrum about this mean value. This variation may be significant for the response of a floating structure, especially at its natural periods.

The variable wind, which influences the damping of the structure dynamics and its slow drift oscillation is considered more important. The variation of wind speed with the vertical elevation is estimated by the following expression:

$$V(1hr, z) = V(1hr, z_R) \cdot \left( \frac{z}{z_R} \right)^{0.125} \quad [21]$$

in which  $z$  = elevation above SWL,  $z_R$  = reference elevation, and  $V$  = wind speed. According to API-RP2A (Eq. 2.3.2-5), the wind frequency spectrum about the 1 hr mean value is described by

$$S(f) = \frac{(\mathbf{s}(z))^2}{f_p \left[ 1 + \frac{15f}{f_p} \right]^{5/3}} \quad [22]$$

in which  $S(f)$  = spectral energy density,  $f$  = frequency,  $z$  = elevation,  $\mathbf{s}(z)$  = standard deviation of wind speed. Various  $f_p$  values may be considered such that it covers the following recommended range indicated below.

$$0.01 \leq \frac{f_p \cdot z}{V(1hr, z)} \leq 0.10 \quad [23]$$

A digital time series for the wind generation is obtained in a manner similar to the wave simulation in a wave basin. An inverse Fourier transformation can be performed to change the wind spectrum from the frequency to the time domain. The wind velocity time series is expressed as below:

$$V(t) = \sum_{i=1}^m v_i \cdot \cos(\mathbf{w}_i \cdot t + \mathbf{f}_i) + V(1hr) \quad [24]$$

in which  $v_i$  = velocity amplitude,  $\omega_i$  = frequency,  $\phi_i$  = random phase angle,  $t$  = time,  $m$  = number of discrete frequency components,  $V(1 \text{ hr})$  = one hour mean wind velocity

The velocity amplitude is defined as:

$$v_i = \sqrt{2 \cdot S(\omega_i) \cdot \Delta\omega_i} \quad (i = 1 \dots m) \quad [25]$$

in which  $S(\omega_i)$  = wind spectral energy density,  $\Delta\omega_i$  = frequency interval. The wind force is calculated from an expression for the Morison drag force:

$$F_{Wind}(t) = \left( \frac{w}{2} \right) |V(t)|V(t) \cdot C_s \cdot A \quad [26]$$

in which  $w$  = density of air,  $V$  = wind speed,  $C_s$  = structure shape coefficient, and  $A$  = projected area of the structure exposed to wind.

An option for the simulation of the variable wind load uses a bank of fans mounted on the carriage facing the superstructure [Chakrabarti (1994)]. The fans are placed at a strategic distance from the model found by a trial and error method. By varying the speed of the fans with time, the wind spectrum may be simulated.

A single variable speed controllable ducted fan (Fig. 5) mounted on the structure platform is an attractive alternative to the bank of fans. This fan models the effect of variable wind loads on the model. The wind speed time history based on the API wind spectrum provides a force time history of the wind loading on the structure. For this purpose, a constant speed variable pitch wind generator with ducting will provide the appropriate center of pressure and spectral wind force desired for tests.

The driving input signal to the wind fan is generated much the same way as the wave generation signal. The wind load time history is measured with the help of a load cell mounted on the model platform between the fan the model. Mean and RMS values for the generated wind load based on the API spectrum is computed and compared with the theoretical predicted wind load. This allows adjustments in the input signal repeating the test until a satisfactory match is found. The input signal may be modified by the feedback signal based on any measured large amplitude of angle of the fan due to the structure motion during the wave run.

#### **4.5 Current Simulation**

In many deepwater locations considerable current may prevail. The effect of current on many deepwater structures may be extremely important. For such structures simulation of current in the wave basin is essential. As mentioned earlier, towing simulates current. However, for many offshore components this may not be adequate.

There are several options in generating local current in the general area of the model in the test basin. These are described in Chakrabarti (1994). Of these, the most desirable is the one where a closed return loop for the flow is provided through the (false) floor of the basin. The water is circulated throughout the width and depth of the basin by ducted propeller. Others are specially built hardware with pumps and manifolds. The are generally

portable and may be installed near the model at any angle. The hardware to generate current is reasonably transparent and has minimum influence on the waves generated simultaneously in the basin.

Some turbulence will be present in the current, which will better simulate the prototype situation and minimize the effect of distortion in the model Reynolds number. It is possible to generate some vertical shear in the current profile (Fig. 6) by selectively throttling the flow.

A thorough calibration of the current generation should be performed before the model is placed in the basin. The current speed should be measured with current meter covering the model neighborhood. Several measurements should be made over this grid to ensure that the current speed is reasonably simulated and the current is reasonably steady and uniform. It should be recognized, however, that a 10-15 percent variation in the current speed is expected.

## **5.0 AREAS OF TESTING**

Certain specific areas of testing required for a floating structure model test are discussed below.

### **5.1 Air Gap Measurement**

The design and location of the decks above the submerged structure depends largely on how the waves influence the run up of water in the vicinity of the structure. The wave impact on the deck is generally avoided in this design. The air gap between the free surface and the deck of the model is measured by mounting wave probes on the model near its submerged surface at the water line. Several wave probes are needed on the model attached to its deck to record the air-gap between the deck and the waves including wave run-up. If possible, resistance (or capacitance) tapes conforming to the shape of the model surface is desired for the air-gap measurement.

### **5.2 Motion Measurement**

The motion measurement may be accomplished by a light mechanical system having linear and angular potential transducers for direct measurement of responses. A non-contacting method, such as an optical tracking system with the associated software is a better alternative for small structures or components. Unlike the mechanical systems, it requires no adjustment in the ballast in the model.

### **5.3 Sectional loads**

Sectional loads (Fig. 7) are often measured on a large semisubmersible by cutting the model through its center in two halves. Three XYZ load cells are attached at the desired points of the hull through its cut to measure the structural loads at these points. The six degrees of freedom loads at these points are determined from these measurements. It is necessary to maintain a small air gap at the cut so that the members do not touch during loading. The gaps for true readings of the load cells are determined from the load cell design and required loads and allow the deflection of the load cells. In-place calibration of the load cells over the expected measurement range should be performed.

The formulation in obtaining the loads at the desired location from the measured loads at the split in the model with the help of three XYZ load cells is derived. A comparison of the measured sectional loads with computations in a test with a semisubmersible is shown in Table 2. In general the racking and shearing loads compared well (mostly within 10 % while some within 20 per cent) with the computed values. The discrepancies at the low periods are large where the measurements may have large error due to the smallness of the loads. There are cases of large discrepancies between the two in the split loads. It is not clear why some of these differences

exist. In this regard it should be noted that the global response of a moored model in the basin compares well with the numerical results as well as is confirmed with field measurements. The local variations, however, produce large discrepancies, such as local pressures, and run-up. This is an area that needs further investigation.

#### **5.4 Towing Tests**

The resistance and the corresponding horse power requirements of a ship under transport in a seaway are routinely determined by means of towing a model of a ship mounted on a carriage in a test basin. The size of tugboats and towing lines that are required for the transportation of an offshore structure to its installation site is also determined in a similar manner.

Offshore structures at their site often experience high current loads during their operation, which may hamper the drilling, and production operation. The current loads on the offshore structure are frequently determined by the simulated towing of its model at the scaled current speeds [OCIMF (1977)].

The direction of current subjected to a moored offshore structure [Kriebel (1992)] may vary with the longitudinal axis of the structure. Therefore, it is customary to test the structure model by towing it at different yaw angles. For all yaw angles the model is rotated with respect to the load cell beam so that the inline axis of the load cell measures the drag load irrespective of the yaw angle. This arrangement is preferred over turning the entire model setup including the towing staff mounted on a PMM rotating ring. While the latter is easier and faster to achieve with the towing carriage equipped with a PMM desired, the former is desirable. In a similar model setup it was found that the towing load on the model introduced an undesirable trim in the model. Even though the towing staffs may be quite stiff, the stiffness of the setup is directly proportional to the stiffness of the load cells, which depends on their design load.

##### **5.4.1 Scaling Up of Towing Load**

The following procedure is applied to scale up to the full scale the resistance measured on a tanker during the towing tests and uses the 1957 ITTC correlation line [Muckle (1987), Chakrabarti (1994)].

- Measure model resistance  $R_m$  at model speed  $V_m$
- Compute total resistance coefficient  $C_{tm}$
- Compute model friction coefficient  $C_{fm}$
- Compute residual coefficient  $C_{rm} = C_{tm} - C_{fm}$
- Add correlation (roughness) allowance  $Ca$  of 0.0004
- Compute prototype ship frictional resistance coefficient  $C_{fp}$
- Add friction coefficient to the residual to obtain total prototype ship resistance coefficient  $C_{tp}$
- Multiply by the normalization factor to obtain ship resistance
- Make correction for the fresh water in model tests
- Compute EHP requirement

The friction coefficient is computed from

$$C_f = \frac{0.075}{(\log_{10} Re - 2)^2} \quad [27]$$

The lateral (drag) force coefficients are determined by normalizing the measured drag force as

$$C = \frac{F}{1/2 \rho L D u^2} \quad [28]$$

where  $F$  is the mean measured force,  $L$  is the model length and  $D$  is its draft, while  $u$  is the mean current speed. The above method for the scaling up the resistance load on a tanker model is routine and has been found to produce good accuracy in determining the ship powering requirements.

#### 5.4.2 Scaling Up of Drag Force

The drag force on a floating structure design [Hoerner, (1965)] is generally evaluated from the basin test of a model of the structure. For the drag force on an offshore structure the scaling problem is similar to the tanker, except the friction formula is not directly applicable. However, a similar method may be proposed.

- Compute drag force on the drag members of the structure at the model speed. Use the  $C_D$  values from the available published data from experiments on these members. This type of information is available for various shapes [Myers, et al. (1968)].
- Correct these values from any shielding effect among the members from the flow. Published data are available on model member shielding (Fig. .8)
- Subtract the computed drag force from the measurement.
- Scale up the residual force using Froude scale.
- Compute prototype drag force using API design guidelines.
- Account for shielding from API design guideline.
- Add drag force to the scaled up data
- Corrections may be made for roughness, density, etc.

#### 5.4.3 Turbulence Stimulator

A series of tests employed a semisubmersible type floating structure subjected to a uniform current. In order to reduce the effect of the laminar flow, the flow field is artificially stimulated to give a turbulent flow in front of the model. The drag coefficients are known to decrease in value as the flow moves from the laminar to the turbulent case. Thus the stimulator is expected to reduce the drag force and produce values close to the expected prototype values. The test results in Fig. 9 provide the average values of the drag forces at the 90-deg yaw angle when the turbulence stimulators are present and without the presence of the turbulence stimulator. At the low end of towing speeds, the stimulator failed to produce appreciable turbulence in the flow and the two cases of with and without become closer. This is evident at the speed of 0.5 ft/s. The effect of the stimulator is clearly seen in the plot. The forces in the presence of the stimulator are considerably lower than those in its absence. This effect is directly attributable to lower values of drag coefficient as found in a turbulent flow experienced by the prototype Reynolds number. Thus the stimulator in effect allows modeling to a more realistic case of flow and reduces the distortion of  $Re$  in a small scale testing.

#### 5.4.4 Towing Vs Current

In another test a tanker model was tested in current [Chakrabarti, et al. (1994)]. In this case the model is moored with soft springs and both uniform and sheared current was generated in the basin. The results on the drag coefficients for different current shears are shown in Fig. 10. These results correspond to a relatively shallow water depth. The resistance in the positive shear (see Fig. 6) is the lowest while that in the negative shear is the highest. Similar findings were made at other yaw angles. It was observed that the flow pattern under the model was quite different (i.e., faster) in the negative shear, which introduced a higher flow separation and may have contributed to the higher load.

This tanker model was tested both as stationary in steady current and in towing. In both cases the model was allowed to heave and roll. The drag resistance was measured in these two cases for the same range of speeds. It was observed during these tests (Fig. 10) in steady current and by towing at similar speeds that towing produced lower values (except at low Re numbers). It implies that towing produces less conservative results for current-induced loads. This is explained physically by examining the flow pattern between the two cases. The observed flow in the two cases is illustrated by the photograph (Fig. 11) showing the same ship shaped structure being towed in still water and being tested stationary in current.

Figure 11 shows the flow around the model in a current test (top) and in a still water towing test (bottom) at the equivalent speeds. The flow during towing shows evidence of standing waves being generated in front of the model. Notice the build-up of the water in front of the towed structure causing a slowdown of flow around the model. Also, during the towing tests the area of flow disturbance and vortices behind the model appear to be larger and less separated from the model. This may have caused a reduction in the drag in towing. Thus one may expect a larger drag load in current compared to the corresponding simulated towing case. The differences in the lateral coefficient  $C$  may be attributed to the observed differences in the flow around the model in the two tests. It should also be noted that current produces some turbulence in the flow approaching the model, which will have similar effect.

### **5.5 Moored System Tests**

The difficulty of modeling and setup of a floating moored system in a basin arises from the following considerations:

- The mooring stiffness is often nonlinear
- The fairlead angle changes with time and loading for a given environment
- The initial angle requires change as different environmental conditions are simulated.

The mooring lines are usually modeled such that the correct non-linear stiffness behavior is achieved at the fair lead connection points. A truncated mooring spread is considered acceptable as long as the stiffness properties at the vessel are correctly represented. It is often important to model all mooring lines individually.

For the success of a small scale testing, it is important that the mooring system simulation is kept simple and the mooring arrangement does not change with every environment. If the pretensioned line force is roughly linear with the line extension, the mooring line may be modeled with a set of linear springs. The springs are chosen such that the stiffness may be easily adjusted to match the linear slope by adding or removing a set of springs. If desired, the mooring line model can be nonlinear. The initial fairlead angle is adjusted in order to match the calculated values. It is understood that this angle will change with loading from the environment. But for large fairlead tension the change of angle will be small. Since there is a large pretension in most cases the error in the angle with load will be small. The initial tensions at the fairleads, which are monitored with the help of the load cell located at the end of the mooring lines at the fairleads are adjusted and maintained.

The above arrangement will allow a model mooring line, which is a set of springs arranged in a straight line, attached to a cable. One end of the cable is attached to the fairlead at the model through a load cell. The other end of the cable is attached to an anchor plate at the bottom of the basin in order to maintain the initial fairlead angle for the particular environment. This attachment point is designed with a pulley system so that the initial angle can be changed from the surface.

The procedure during testing is as follows. The model is moored with the straight line mooring system with the initial fairlead angles and the ballasted anchor plates set at pre-marked locations at the basin floor. For the test

runs where steady loads are needed, the load will be applied with the line and pulley arrangement. The model will displace in the aft direction under this load. The model will be pulled back to its initial position by the anchor lines to its initial position (marked on the carriage). This will maintain the initial position while pretensioning the mooring lines.

In order to simplify setup changes, the anchor plates may remain at the same locations between the test runs with different drafts. Note that the initial fairlead angles will be different under this arrangement as in the real case. The anchor plates can be re-located for different heading angles.

Regarding the measurement system, particularly the motion measurement system, the carriage with the instrumentation system is positioned after the pretension displacement of the model has taken place. This will allow the measuring system to stay within the limits of motion of the model from the wave and slow drift oscillations.

This method of testing moored system has been found to match the numerical results from the hydrodynamic interaction programs. Some evidence of correlation with the field experience on the global response also exists.

### **5.6 Second Order Slow Drift Tests**

The second-order wave forces on a floating vessel due to regular waves are proportional to the square of the wave height. In addition to the steady drift force, a slowly oscillating drift force is generated on a moored floating structure due to an irregular wave. This drift force is excited around the long natural period of the system from the difference frequencies in the irregular wave components. Thus a low frequency response of the vessel is expected covering the frequency band around the natural frequency of the system. This response spectrum due to a random wave is related to the wave spectrum through an integral in terms of a quadratic transfer function.

It is difficult to establish the values of this quadratic transfer function through the spectral approach. Therefore, the following technique is recommended to develop the quadratic transfer functions for the slow drift motion. Since the slow drift motion appears as the difference in the frequencies in the irregular wave and has a bandwidth around the natural frequency of the system, this bandwidth can be established from the irregular wave runs. Then frequency pairs can be chosen from the input wave spectra such that they produce a difference frequency in this band. This will give rise to a symmetric matrix of the pairs of wave frequencies. Wave groups from the frequency pair of equal amplitude are generated in the basin with these frequency pairs and the responses are measured. The low frequency components are filtered through FFT and the response amplitudes are derived. These response amplitudes are normalized with respect to the wave amplitude squared.

It should be kept in mind that this technique of measuring the response and deriving the quadratic transfer function requires the derivation of the damping characteristics of the system at different frequencies. It is expected that the damping characteristics of the system will not alter appreciably by changes in the mooring system. However, the model damping may not be scalable to the prototype damping. Since the amplitude of the slow drift oscillation is directly proportional to the damping, it is difficult to predict slow drift from the model tests. They can be used to validate the design tool, which can then be adjusted for the prototype calculations.

The data reduction procedure for the quadratic transfer function is similar to the RAO computation except for the normalization method. It is established that the slow drift is proportional mostly to the square of the group wave amplitude. The matrix of the quadratic transfer function is generated from the wave group test runs. These values are then used to compute the slow drift response spectra. The computed response spectra can then be compared with the measured spectra in the irregular waves.

## **6.0 CONCLUDING REMARKS**

In spite of the many limitations of small scale deep water testing in a model basin discussed here, a properly designed model test generates invaluable insight into the performance of the system and provides guidance for the development and verification of the numerical tool that is used in the design of such a system. Numerical wave tank can not fulfill this insight especially for such systems in a virgin territory. It may sometimes be advisable to test the various components of an offshore structure for specific insight into the hydrodynamic and structural response at different scales in sequence before testing the complete system.

There are several scaling laws that are encountered in planning a model test. The formulation of these laws and the scaling factors are explained. Their importance in a particular structure model is discussed.

Several aspects of testing a ship or offshore structure model have been investigated. The available facilities and their dimensional limitation have been given. Various methods of simulating the environment in the model basin have been discussed. The measurement and scaling of resistance of a floating structure under tow or in an ocean current in an offshore model basin has been shown.

Several methods of obtaining the important localized effect of waves on a structure are discussed. The air-gap between the under deck and the free surface and the section load measurement on a floating structure is demonstrated.

Some practical methods in remedying the modeling deficiencies are given. It is clearly shown that a simple grid system towed in front of the model covering its width and draft creates a turbulence, which produces a significant change in the drag load partially correcting the distortion in the Reynolds number scaling in a small scale test.

A test was run with a moored tanker model in current and then repeating the test by towing the model in still water in which the model was allowed to heave and roll similar to the moored case. The towing test produced lower drag coefficient compared to those in the equivalent steady current. This observation may have direct implications for such type of modeling.

It is hoped that the results presented in this paper will help test basin and test engineers determine a better suited testing and data reduction technique for a floating offshore structure model.

## **7.0 REFERENCES**

Anon., "Floating Production Systems Proliferating Around the World", Oil and Gas Journal, Dec. 7, 1992, pp. 18-24.

Bendat, J.S. and Piersol, A.G., Engineering Applications of Correlation and Spectral Analysis, John Wiley & Sons, New York, 1980.

Chakrabarti, S. K., Offshore Structure Modeling, World Scientific Publishing, Singapore 1994.

Chakrabarti, S. K., A. R. Libby and P. Palo, "Small Scale Testing on Current Induced Forces on a Moored Tanker," Ocean Engineering, Elsevier, 1994.

Edwards, B., "The Future of Floating Production", Offshore, Oct., '96, pp. 120.

Hoerner, S. F., Fluid-Dynamic Drag, Published by the author, 1965.

Kriebel, D., "Viscous Drag Forces on Moored Ships in Shallow Water", US Naval Academy Report, Annapolis, MD, 1992.

Muckle, W., Muckle's Naval Architecture, Butterworths, London, 1987.

Myers, J.J., McAllister, R.P., and Holm, C.H., Handbook of Ocean and Underwater Engineering, McGrawHill, New York, 1968.

Oil Companies International Marine Forum, "Prediction of Wind and Current Loads on VLCC's", London, UK, 1977



**TABLE 1. SELECTED DATABASE ON AVAILABLE TEST BASINS SUITABLE FOR DEEP WATER TESTING**

<b>FACILITY</b>	<b>LENGTH X WIDTH X DEPTH</b>	<b>DEPTH OF DEEP SECTION</b>	<b>WAVE</b>	<b>CURRENT</b>	<b>WIND</b>	<b>TOWING</b>	<b>PMM</b>
DHI, Denmark 45 76 95 55	30m x 20m x 3m	12 m	0.5-4 s multi-directional	local	fans	yes	no
DMI, Denmark 45 45 87 93 25	240m x 12m x 5.5m	none	0.5-7 s	towing	fans	yes	no
DTMB, US Navy, MD (MASK) 202-227-1515	79.3m x 73.2m x 6.1m	none	0.5-3 s multi-directional	not known	fans	yes	yes
DTMB, US Navy, MD (Deep Basin)	846m x 15.5m x 6.7m	none	1-3 s	towing		yes	yes
IMD, Newfoundland 709-772-4797	200m x 12m x 7m	none	0.5-10 s multi-directional	local	fans	yes	yes
MARIN, Netherlands (Seakeeping) 31-317-493911	100m x 24.5m x 2.5m	6 m	0.7-3 s	none	fans	yes	yes
MARIN, Netherlands (Wave + Current Basin) 31-317-493911	60m x 40m x 1.2m	3 m		0.1-0.6 m/s	fans	Not known	Not known
MARIN, Netherlands (Planned Offshore Basin)	46m x 34m x 10.5m	none	multi- directional; both directions	shear current; false bottom		Not known	Not known
MARINTEK, Norway 47-735-9500	80m x 50m x 10m	none	Irregular	0.2 m/s	fans	no	Not known
NRC, CANADA 613-993-6653	Ottawa, 50m x 30m x 3m	5 m	multi-directional	local	fans	no	no
OMB, Escondido, CA 619-737-8850	90m x 14.6m x 4.6m	9 m	0.7-4 s	local, towing	fans	yes	yes
OTRC, Texas A&M 409-845-6000	47.5m x 30.5m x 5.8m	16.7 m	0.5 - 4 s multi-directional	local	fans	Not known	no
USNA, Annapolis, MD	80m x 10m x 5m (approx.)	none	0.5-10 s	none	none	yes	yes

Table 2 . Section Loads On Split Semisubmersible

	<b>Split</b>	<b>Force</b>		<b>Racking</b>	<b>Force</b>	
<b>Wave Per.</b>	<b>Calc.</b>	<b>Test</b>	<b>calc / test</b>	<b>Calc.</b>	<b>Test</b>	<b>calc / test</b>
<b>sec</b>	<b>lbs</b>	<b>lbs</b>		<b>lbs</b>	<b>lbs</b>	
<b>6</b>	<b>4.57E+06</b>	<b>1.75E+06</b>	<b>2.620</b>	<b>1.83E+05</b>	<b>2.94E+05</b>	<b>0.622</b>
<b>8</b>	<b>1.46E+06</b>	<b>6.18E+05</b>	<b>2.369</b>	<b>1.83E+05</b>	<b>1.96E+05</b>	<b>0.933</b>
<b>10</b>	<b>1.28E+06</b>	<b>9.03E+05</b>	<b>1.419</b>	<b>1.83E+05</b>	<b>1.96E+05</b>	<b>0.933</b>
<b>12</b>	<b>1.83E+05</b>	<b>3.92E+05</b>	<b>0.466</b>	<b>1.83E+05</b>	<b>1.96E+05</b>	<b>0.933</b>
<b>14</b>	<b>1.83E+05</b>	<b>2.94E+05</b>	<b>0.622</b>	<b>1.83E+05</b>	<b>1.67E+05</b>	<b>1.097</b>
<b>16</b>	<b>3.66E+05</b>	<b>3.63E+05</b>	<b>1.008</b>	<b>1.83E+05</b>	<b>1.96E+05</b>	<b>0.933</b>

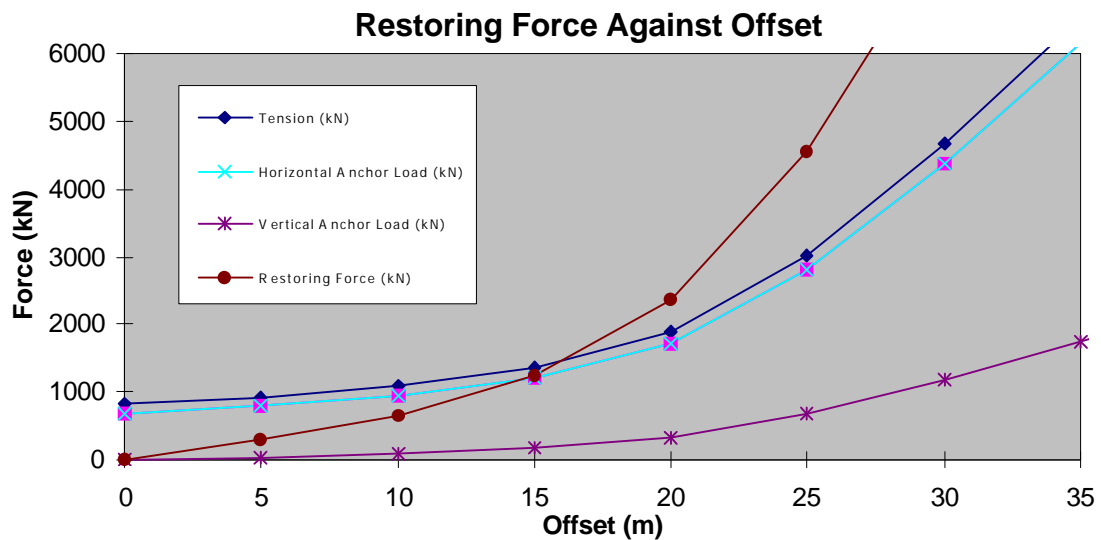


Fig. 1 Mooring Line Stiffness to be modeled in the Basin

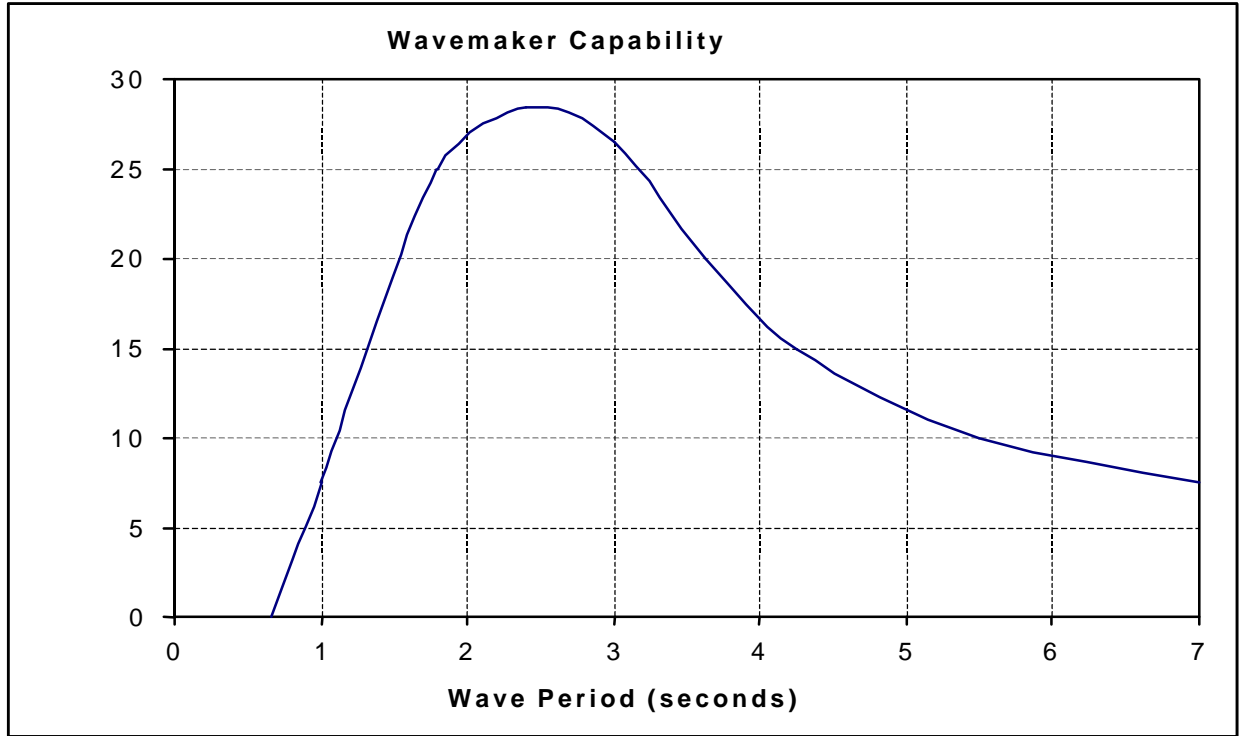


Figure 2 Wave Making Capability at OMB

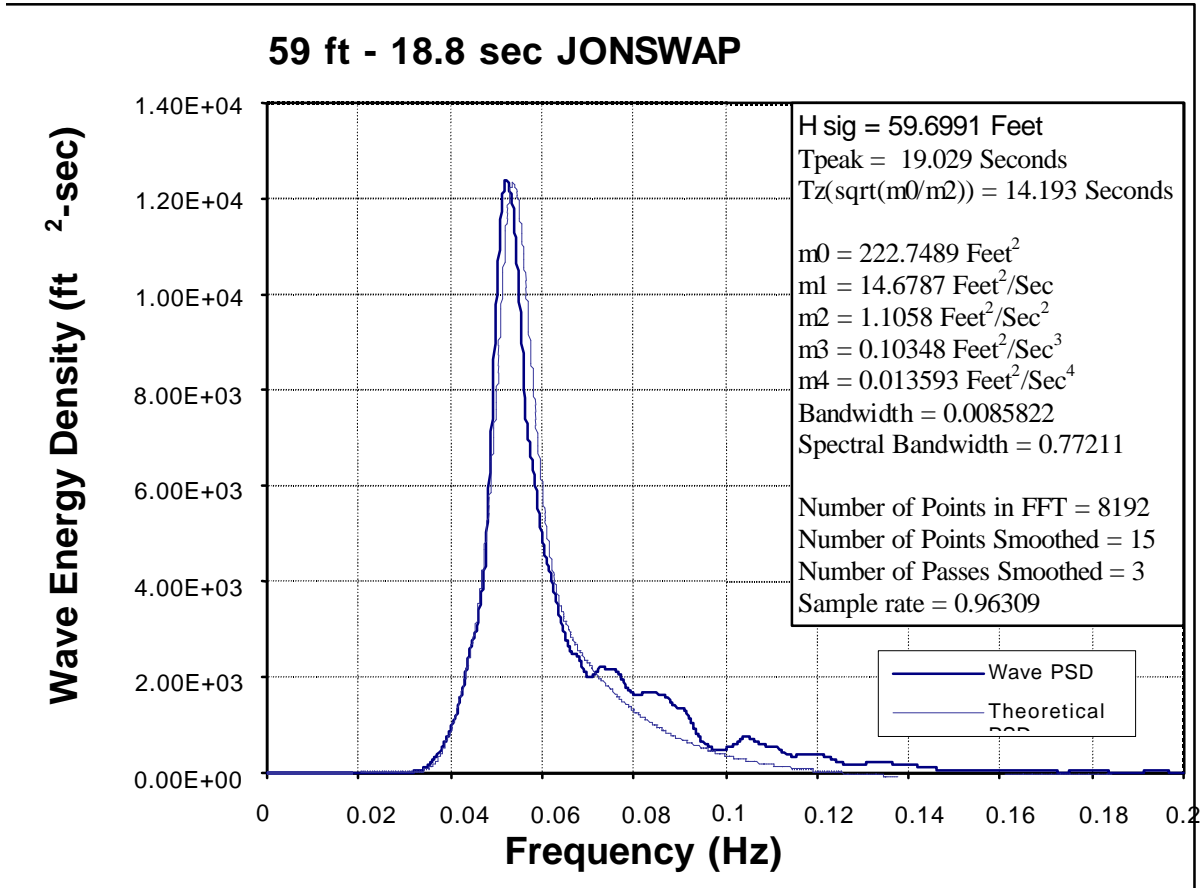


Figure 3 Generation of a JONSWAP Spectrum

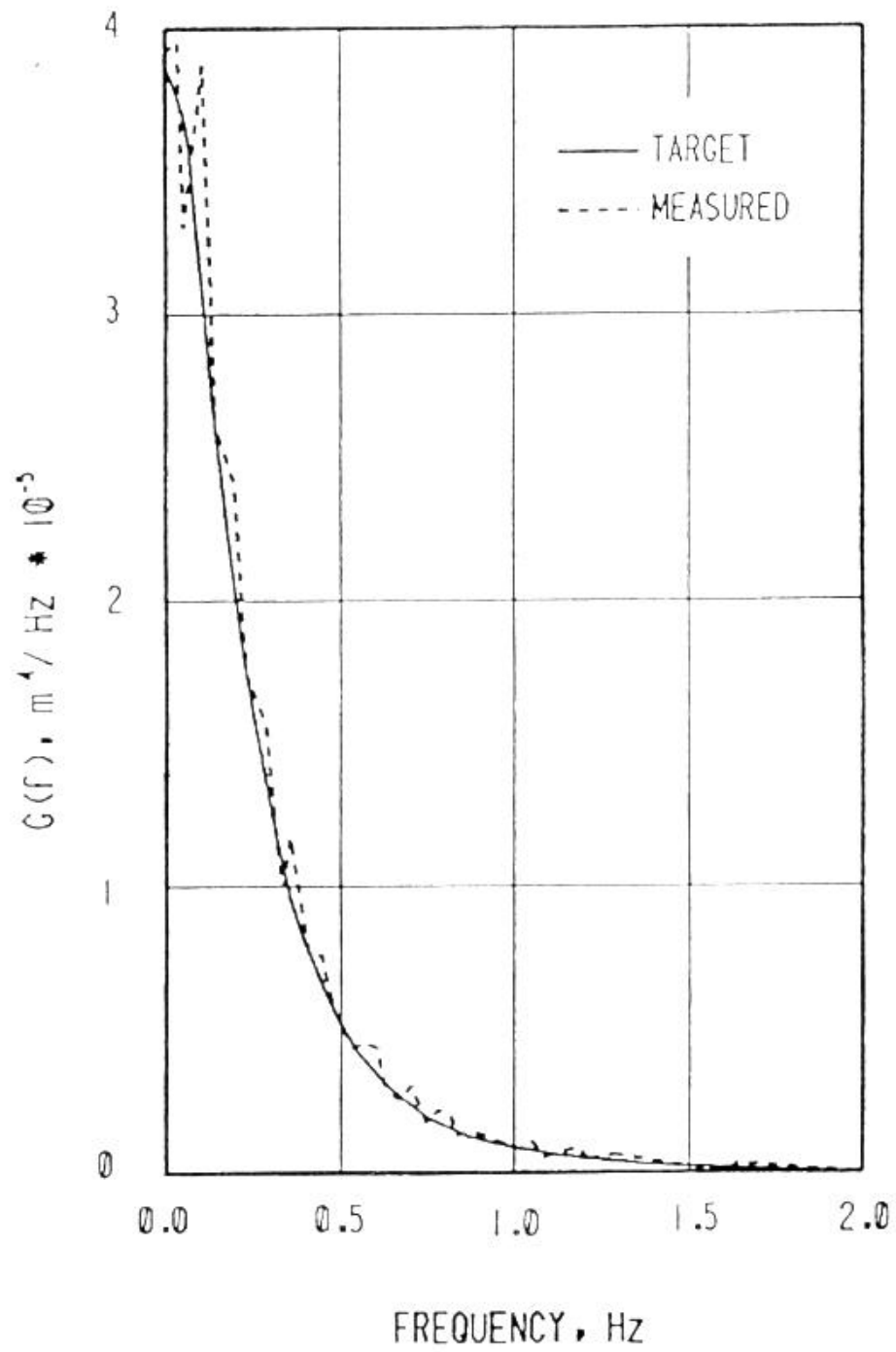


Fig. 4 Comparison of the groupiness function for a JONSWAP wave

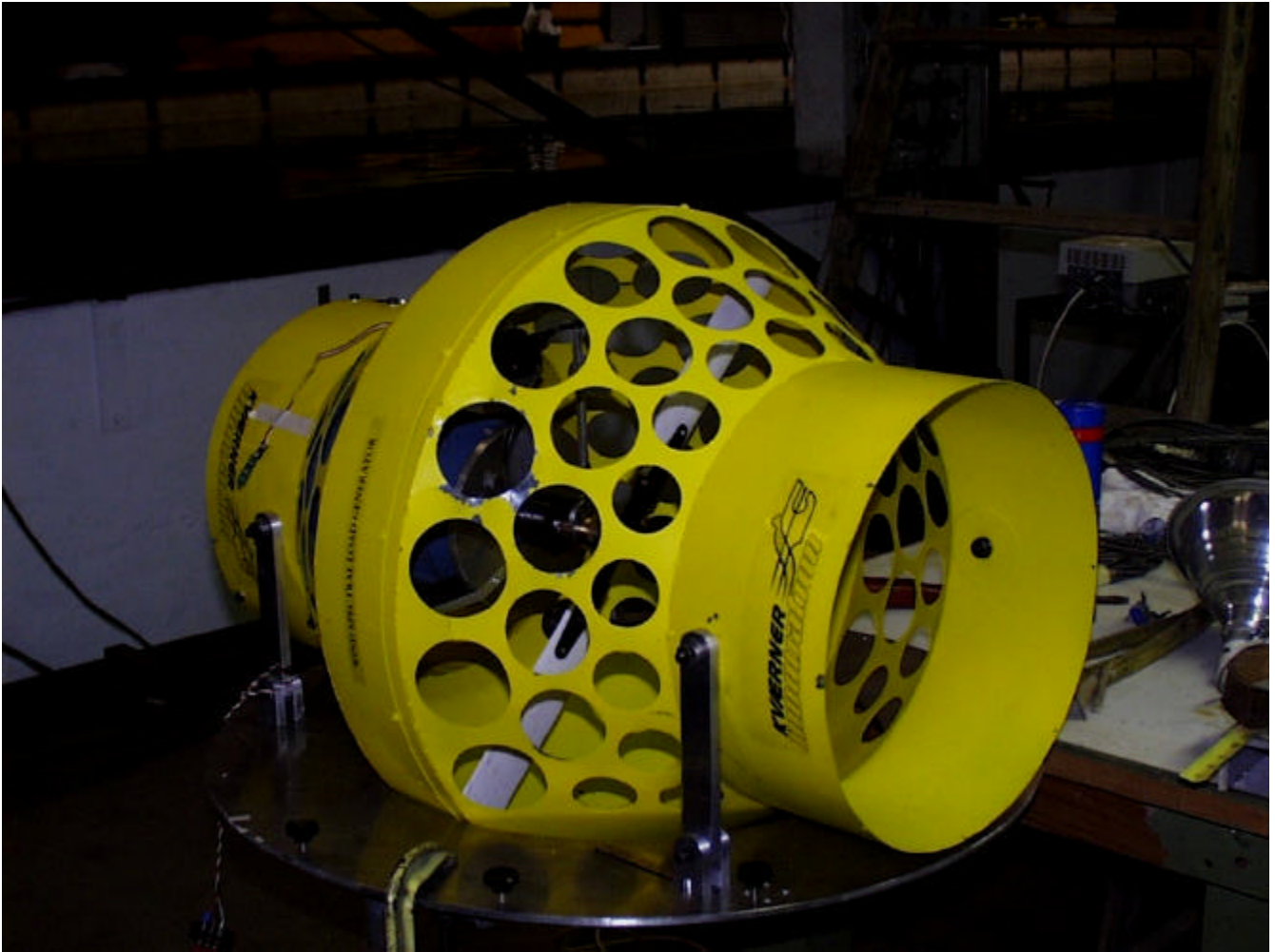


Fig. 5. Ducted Fan for Simulation of Wind Load

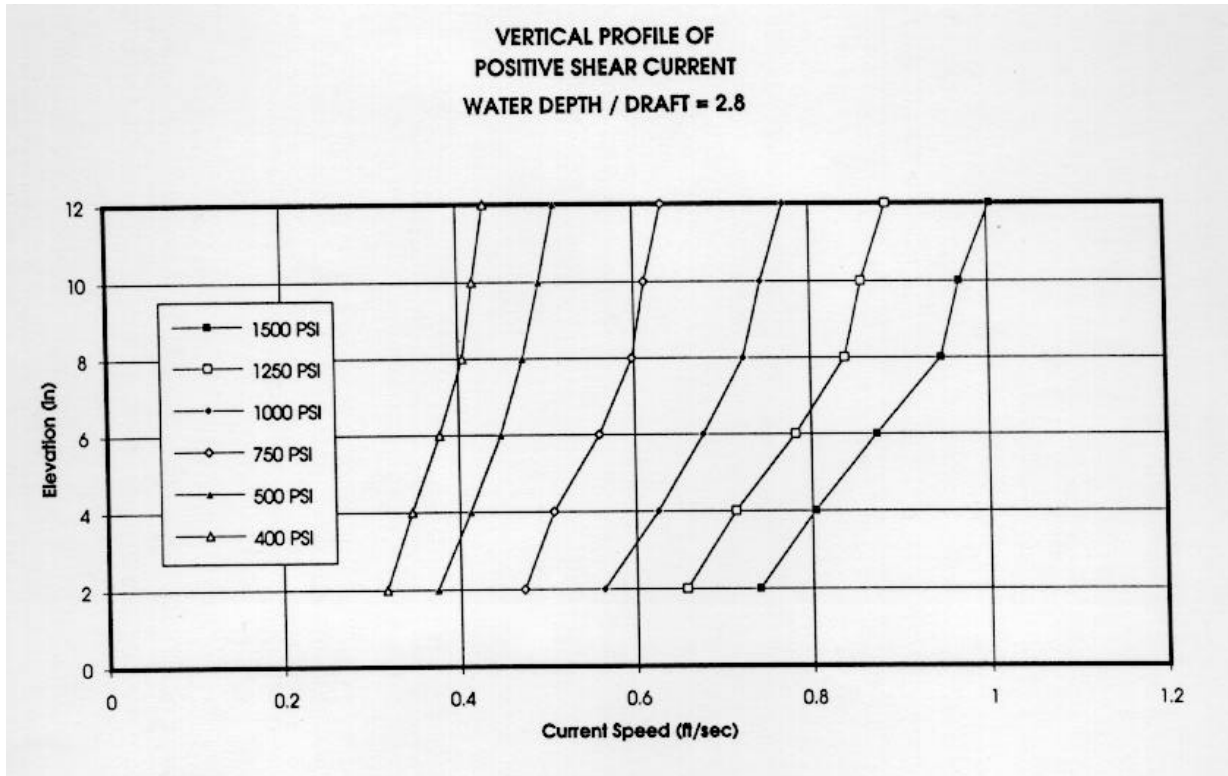


Fig. 6. Shear Current Generation Technique in Wave Basin



Fig. 7 Sectional Load Measurement Technique on the Hull of a Moored Floating Structure in a Seakeeping Test

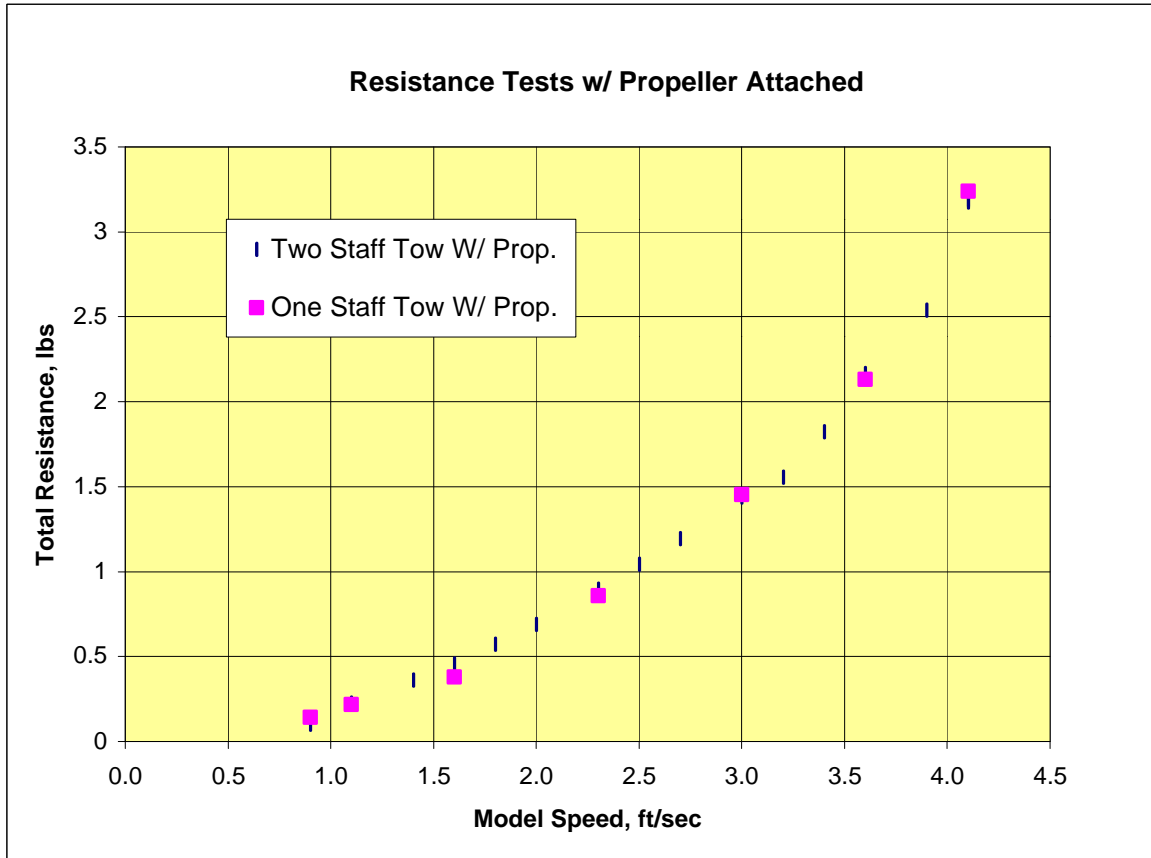


Fig. 8. Measured Resistance Load versus Measured Speed on NNS Calibration Model

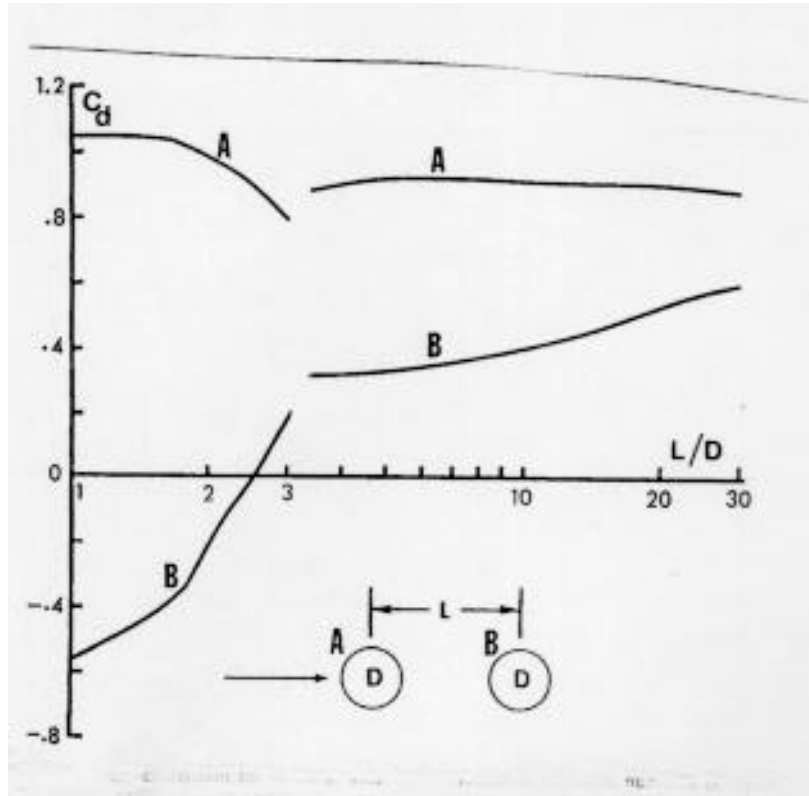


Fig. 9 Shielding Effect on Two Tandem Cylinders in Current

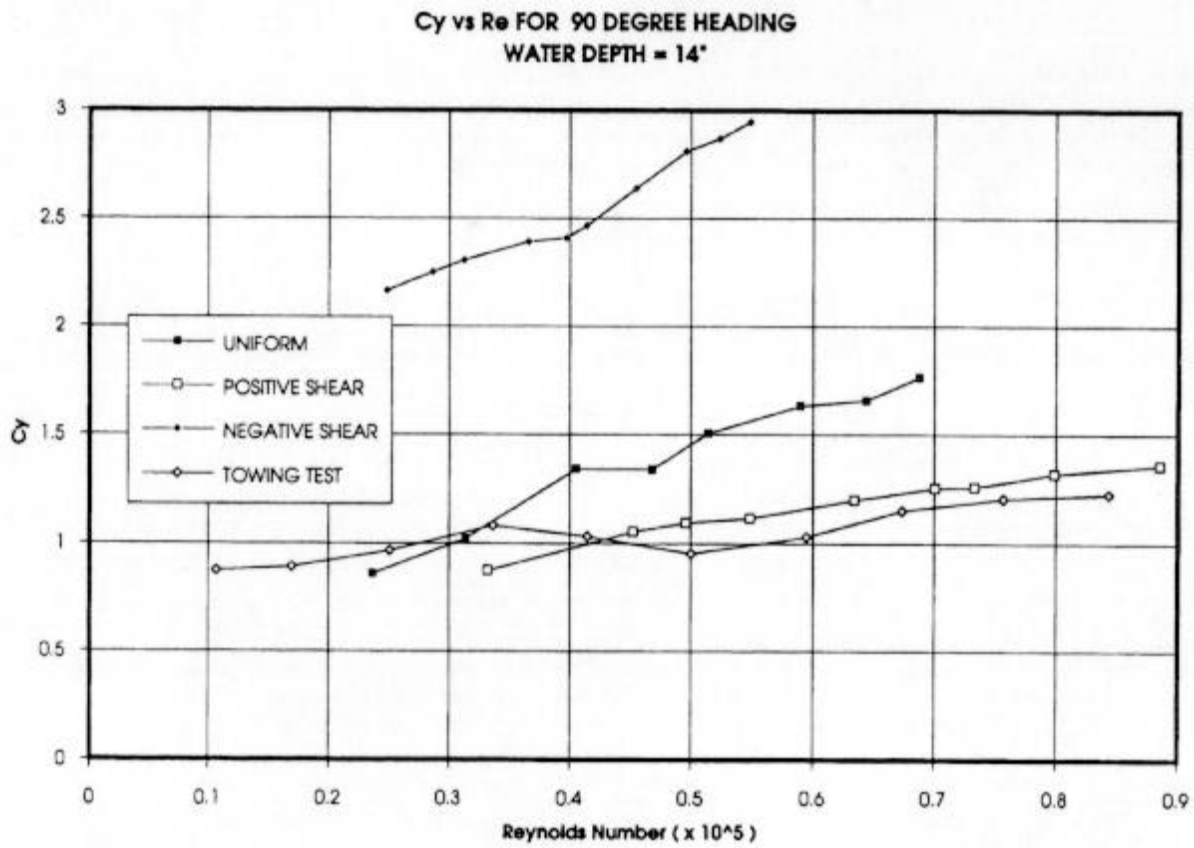


Fig. 10 Drag Load on a Tanker Model in Shear Currents and Under Tow

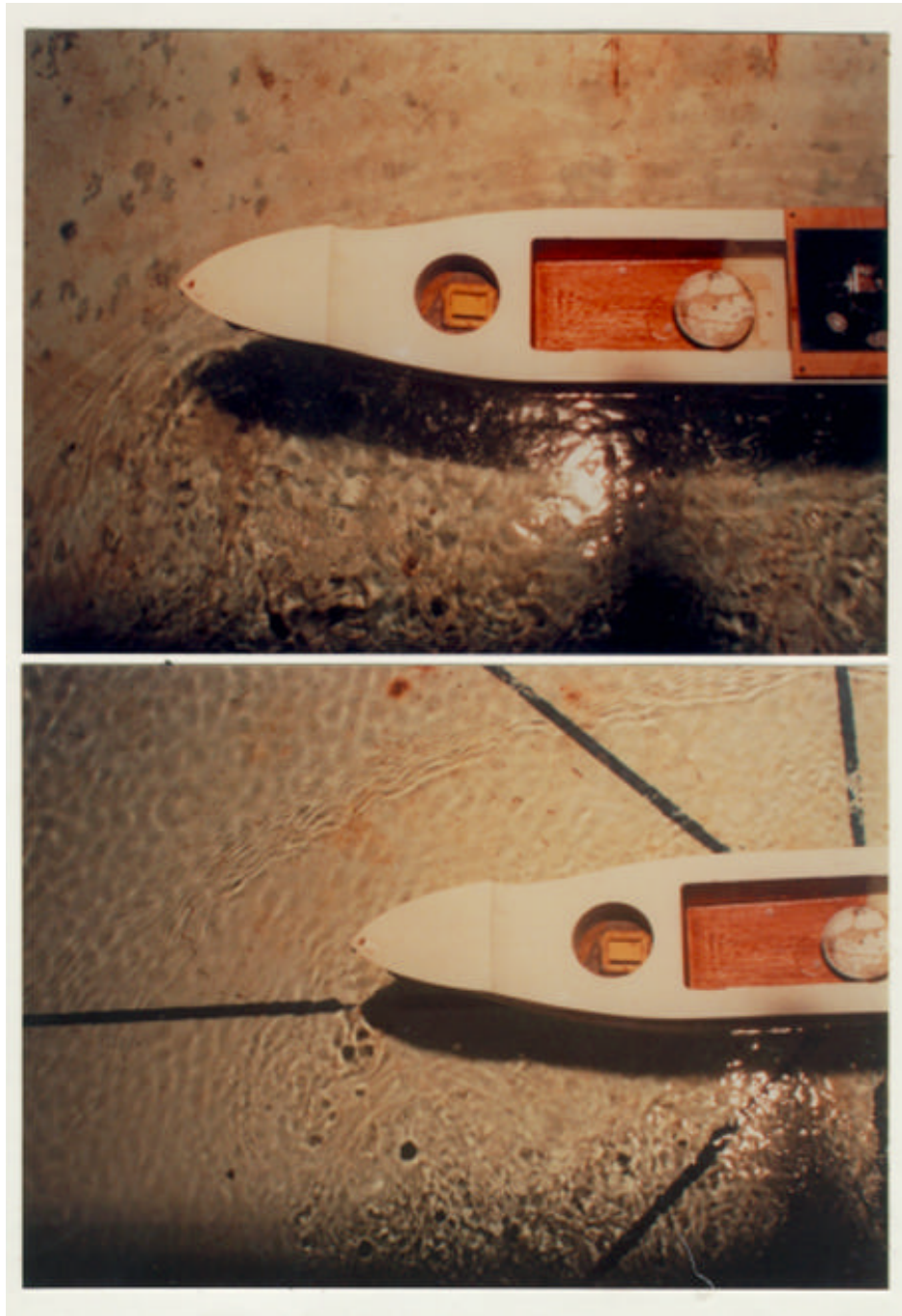


Fig. 11 Flow Effect Around a Tanker (a) Under Tow and (b) in Uniform Current at Same Speed

